AENSI Journals
Advances in Environmental Biology
ISSN:1995-0756 EISSN: 1998-1066
Journal home page: http://www.aensiweb.com/aeb.html

Morphological synthesis and environmental application of ZSM-5 zeolite crystals from combined low-water and fluoride syntheses routes

[1]Mutiu K. Amosa, [1]Ma'an F.R. AlKhatib, [1]Mohammed S. Jami, [1]Dzun N. Jimat, [2]Owolabi, R. Uthman, [1]Suleyman A. Muyibi

[1]Department of Biotechnology Engineering, Kulliyyah of Engineering, International Islamic University Malaysia.
[2]Department of Chemical Engineering, University of Lagos, Nigeria.

ARTICLE INFO

Article history:
Received 14 Feb 2014
Received in revised form 24 February 2014
Accepted 29 March 2014
Available online 14 April 2014

Key words:
ZSM-5 crystals, Morphology, Adsorption, Petroleum Effluent, Si/Al Ratio

ABSTRACT

ZSM-5 crystals have been morphologically prepared through the combination of Fluoride and Low-Water Synthesis Routes. This was done in order to bring about larger zeolite crystals with high Si/Al ratio and surface area suitable for environmental applications. The zeolite was analyzed to have crystal size between 200 – 218µm with a micropore volume of 0.79cm^3/g. It was also found to possess a Si/Al ratio (SAR) of 194.4 with good adsorption and catalytic prowess when analyzed by SEM and XRD. The prepared zeolite was employed in the petroleum refinery wastewater treatment to evaluate its organic and inorganic removal efficacies as evident from the Chemical Oxygen Demand (COD) and Iron (Fe) contents adsorption where it exhibited 99% and 98% efficiency removal respectively.

To Cite This Article: Mutiu K. Amosa, Ma'an F.R. AlKhatib, Mohammed S. Jami, Dzun N. Jimat, Owolabi, R. Uthman, Suleyman A. Muyibi., Morphological synthesis and environmental application of ZSM-5 zeolite crystals from combined low-water and fluoride syntheses routes. ***Adv. Environ. Biol., 8(3),*** *613-625, 2014*

INTRODUCTION

For the communities living close to crude oil exploration and/or processing sites, environmental quality and sustainability are fundamental to their overall wellbeing and development. According to UNDP, more than 60 per cent of the people in those regions usually depend on the natural environment for their livelihood. For many, the environmental resource base, which they use for agriculture and/or fishing, is their principal or sole source of food. The major pollution that usually leads to environmental damages of these livelihood resources is that water. Therefore, pollution poses significant risks to these human rights [1,2,3]. In order to mitigate these various pollutions in our environments, various methods of treatment have been devised and one of the prominent amongst them is adsorption process. It is observed that the most commonly employed crystalline materials for liquid adsorptive separations are zeolite-based structured materials [4].

The past six decades have seen a phenomenal and chronological progression in molecular sieve materials from the aluminosilicate zeolites to microporous silica polymorphs, microporous aluminophosphate-based polymorphs, metallosilicate and metallophosphate compositions, octahedral-tetrahedral frameworks, mesoporous molecular sieves,

Zeolites among other definitions, are crystalline aluminosilicates with a three-dimensional framework structure that forms uniformly sized pores and cavities of molecular dimensions making them suitable for wide use in the industry for catalytic, sorption and ion-exchange applications. The types of assembly of cavities or channels in zeolite structures control the size of micropores, orientation of microporous channels, and the morphology of zeolite particles [5]. Morphology is originally related to the framework type and also closely related to the micropore size, crystal size, and shape, and directly affects the physicochemical properties of zeolites [5], making them suitable for wide use in the industry for catalytic, sorption and ion-exchange applications. In the nanotechnology world of today, zeolites have ceased to be minerals merely displayed in museums, and have become a commercial and scientific success-story since their large-scale utilization in industry [6]. Besides the natural types of zeolites, synthetic ones continued to spring out from various laboratory researches around the world to be applied in refining, environmental, polymer and chemical industries. Amongst other porous materials being employed commercially, zeolites have made an unprecedented impact in several industrial processes such as catalysis, adsorption, ion-exchanging, etc.

Corresponding Author: Ma'an F.R. AlKhatib, Department of Biotechnology Engineering, Kulliyyah of Engineering, International Islamic University Malaysia
Phone: +603 6196 4553, +601 6236 5704; Fax number: +603 6196 4442;
E-mail: maan@iium.edu.my, dhakisalafi@live.com

From the scientific point of view, majority of the base chemicals constituting our daily consumers goods and energy carriers like transportation fuels have passed through the micro- and mesopores of molecular sieves. Some zeolite structures, mainly MFI and FAU are very resourceful materials with the potentials of fine-tuning their properties to meet particular requirements of diverse industrial applications [6].

Faujasites (X, Y) and other zeolites (A, ZSM-5, beta, mordenite, etc.) are the most popular zeolite materials [4]. The Faujasites are recognized as zeolites used as adsorbents, ion exchangers and catalysts [7]. Due to their larger sizes and pores and unlike the MFI-type framework, the FAU- and LTA-type zeolites are not expected to be affected by crystal morphology fine-tuning as a result of the three-dimensional channel systems they do possess. MFI zeolites such as ZSM-5 on the other hand has high porosity which makes it suitable for gaseous and aqueous phases' adsorption. This is due to their narrow pore size distribution and the ability to fine tune their physicochemical properties such as Si/Al ratios, water content, ion exchange capacities and acidic-basic properties. MFI--type zeolite possesses two intersecting pore structures. The minor and major axis dimensions are respectively, 5.1 × 5.5Å for sinusoidal channels and 5.3 × 5.6Å for the straight channels. Because of this, we prefer to introduce morphological synthesis to ZSM-5 which is a member of the MFI family. With some dependency on structure directing agents (SDAs), pre-cursors, mineralizers, there are reports that MFI-type zeolites with various crystal shapes have been prepared [8,9,10,11,12,13]. However, the reported crystal sizes are less than 100 µm.

Water content of the synthesis mixture could also play prominent role in the final product's morphology as it can modify the structure directing agent (SDA) involved in the synthesis and thus, the pore architecture and morphology of the resulting zeolite will be affected [14].

SDAs which is usually referred to as the *"templates"* are the quaternary ammonium chemicals responsible for the space filling, structure directing and true templating that are often located in channels and cages. The microporosity of zeolites is generated by the incorporation of pore-generating species (*porogens*) such as alkyl-ammonium molecules, which compensate negative charges on the crystallizing silicate framework. Several of such species (*porogens*) can also aggregate to generate pores that are larger than those produced by non-aggregating *porogens* [15]. Though there are arguments that TPAOH is not a template in its true sense because of the inconsistency in its symmetry and channel, and incomplete structural control between the encapsulated TPAOH and the framework, there are however reports indicating that TPAOH can successfully assisted in synthesizing large surface area zeolites [16,17,18,19], either when singly or co-employed with another template (*co-templating*).

The Si/Al ratio of a zeolite may be controlled by the composition of the synthesis solution used for the zeolite synthesis. Increase in the Si/Al ratio increases the adsorption capacity of the zeolite. The degree of hydrophobicity, which increases with increasing Si/Al ratio of the structure, determines a zeolite's suitability for the removal of organic contaminants from aqueous solutions [5,6,19,20,21]. The polarity of such zeolite could then be adjusted through the change in the Si/Al ratio. A lower Si/Al ratio gives a more hydrophilic zeolite capable of adsorbing polar molecules stronger. Subsequently, charged zeolite frameworks have counter ions present in the zeolite pores, which may affect both the adsorption properties and the effective pore size of the zeolite. High Si/Al also enhances zeolites' hydrothermal stability. A larger counter ion results in a smaller effective pore size, the property can thus be tailored through the replacement of those counter ions by ion exchange [7]. MFI-type zeolites such as ZSM-5 and Silicalite-1 are highly siliceous with Si/Al ratios ranging from about 10 to infinity and in principle, the higher the Si/Al ratio the easier the synthesis. Hydrophobicity and organophilicity of MFI zeolites made them useful in the removal of organics from water steams besides their stabilities for separations and catalysis in the presence of water. Due to these high Si/Al ratios, most of the cation sites are in the MFI channels and all changes to cation number and type can affect the adsorption properties. Except for Silicalite-1 which is completely siliceous without any aluminum framework, ZSM-5 and others have been observed to possess increase in adsorption capacity as the Si/Al ratio increases. The adsorption capacity of alkanes in MFI has been found to increase with decreasing non-framework cation density (increasing Si/Al ratio) as reported by [4].

Through these aforementioned property adjustments, a number of synthetic zeolitic materials with different frameworks have been reported. The most pertinent parameter controlling the properties is the structure and the Structure Commission of the International Zeolite Association (IZA) has approved up to 213 zeolitic framework type codes [22] with frameworks of varying significant pore sizes.

Various zeolite synthesis methods ranging from the fundamentally and conventionally known hydrothermal method to ionothermal, solvothermal, microwave assisted, low-water, to Fluoride methods have been reported. Although, the most common mineralizer for silica-based zeolites is the hydroxide ion OH^-, it has been discovered that replacement of the hydroxide anions by Fluoride anions has made it possible to obtain zeolites even in slightly acidic media (pH ≈ 5). At such pH values the solubility of silica increases significantly in the presence of fluoride because of the formation of hexafluorosilicate SiF_6^{2-} species. Fluoride could improve mineralizing and coordination activities during synthesis besides its ability to result in highly stable siliceous zeolite structures with less defects whereas the transition metal ions hydrolyze to form hydroxides or oxide

precipitates in high pH solutions [5,7,21]. Large perfect single crystal formation is greatly enhanced between 10 – 80 µm and the crystals obtained are usually of good quality with sizes generally exceeding the values obtained in alkaline type synthesis. Each of the synthesis methods has its advantages depending on the properties sought in the product.

The synthesis of large zeolite single crystals is of great interest for a large number of requirements, comprising single-crystal structure analysis; fine-structure analysis; study of crystal growth mechanisms; study of adsorption and diffusion; and the determination of anisotropic electrical, magnetic, or optical properties [5]. Small zeolite particles are factually recognized for their high surface area especially in heterogeneous catalysis, it is however an established fact that higher selectivity is offered by larger crystallites because their internal surface area accounts for a much greater proportion of the total zeolite surface area which is as a result of formation of complex composite building units (CBUs), such as rings, through the continuous linking of basic building units (BBUs) also called tetrahedrons [5,23,24]. For adsorption and/or catalytic processes to be productive, the molecules of interest need to diffuse to adsorption/catalytic sites as quickly as possible thus larger crystals give better and quicker diffusion into adsorption or catalytic sites [25,26]. Furthermore, a larger crystal zeolite with relatively large internal and external surface area will remove contaminants from wastewater. The combination of Low-water and Fluoride routes with good choice of SDA usually brings about the development of relatively large crystals of shape-selective zeolites due to their internal surface area accounting for much greater proportion of the total zeolite surface area [7].

Here, we report the morphological synthesis of a 10-member-ring ZSM-5 zeolite through the exploitation of combined advantages in Fluoride and Low-Water synthesis routes, as extensively explained above, to attain better adsorptive and shape selectivity capacities. Besides, the efficacy of the zeolite in the adsorptive removal of petroleum effluent/wastewater contaminants in meeting the threshold set by the [27] was also presented in this study.

Experimental Section:

Materials and Equipment:

The reagents used in the zeolite synthesis were tetrapropylammonium hydroxide – (TPAOH, 98wt%, Aldrich), tetrapropylammonium bromide (TPABr, 98wt%, Aldrich), Silica Sol (40wt%, Silica), Alumina (Al_2O_3, 88wt% Aldrich), HF (95%, Aldrich), Sodium Hydroxide (NaOH, 98wt% Aldrich), and deionized water.

X-ray diffraction (XRD) patterns are obtained with a 1.54Å Siemens D500 diffractometer with a monochromatic Cu K α source. AimSizer 11 (0.1 - 500µm) particle analyzer was used and the scanning electron microscope (SEM) images were also taken on a Philips XL-30 electron microscope operated at 20kV for product characterization.

Synthesis and Characterization of ZSM-5 Zeolite:

The zeolite ZSM-5 was prepared following the *IZA Verified Synthesis for ZSM-5* [30] with little modification. The overall molar composition for the synthesis mixture was $6Al_2O_3$: $80(TPA)_2O$: 40HF : $8Na_2O$: $220SiO_2$: $400H_2O$. The silica precursor and template were mixed for 10 minutes and the resulting clear solution was added to a mixture of alumina precursor and deionized water. The whole mixture was stirred for 6 hours in order to attain homogeneity after which HF (mineralizer) was added and then stirred. All these were done in polypropylene containers. The final mixture was then emptied into a simple standard steel autoclave with a Teflon liner from Parr Instruments and placed in an oven at 170 ^{O}C for 3 days to attain crystallization. The solid product was oven-dried till constant weight before it was calcined at 550 ^{O}C for duration of 6 hours in a tube furnace in order to release the quaternary ammonium salt used as structure directing agent and the fluoride used as mineralizer from the pores formed. The product was allowed to cool down to room temperature, the crystals thus obtained were washed with distilled water and dried at 100 ^{O}C.

Adsorption Studies:

The liquid petroleum refinery effluent was collected from Nigerian Petroleum Refining Company (NPRC) now Nigerian National Petroleum Corporation (NNPC) at Alesa-Elema near Port Harcourt, Nigeria and the physico-chemical characteristics (Table 1) of the wastewater (effluent) were determined following the chemical analytical procedures described by [28,29). Batch adsorption was carried out by splitting the refinery wastewater into 50 ml samples. One was kept as reference and the others were treated using varying dosage of zeolite from 0 – 120 mg at 30 minutes adsorption time. 100 mg dosage was also tested at various adsorption times of 0 – 100 minutes. Each sample was batch-shaked for 30 minutes using a magnetic stirrer. The experiments were performed in triplicates and the averages recorded. The sample was then paper filtered and analyzed to determine the residual contents of the adsorbates.

Table 1: Physico-chemical characteristics of the petroleum effluent

Parameters	Average Value	Department of Petroleum Resources (DPR) Limit
Temperature (^{0}C)	34	35
pH	5.5	8.5
Turbidity (NTU)	1100	10
TSS (mg/L)	1200	50
COD (mg/L)	1100	40
Total Fe (mg/L)	5.5	1.0
Cr^{4+} (mg/L)	0.5	0.03
Cu^{2+} (mg/L)	0.4	1.0
Zn^{2+} (mg/L)	1.2	1.5
Pb^{2+} (mg/L)	1.0	0.05

RESULTS AND DISCUSSION

Fig. 1 represents the XRD analysis of the calcined ZSM-5 zeolite. The XRD patterns obtained, in terms of their peak positions and relative densities were found to be in correlation with those found in [30]. It is advised that the formation of large crystals become more probable if the rate of nucleation is very low and the observation from this study shows that a long crystallization period is indispensable in large zeolite crystals synthesis. The XRD spectra showed a well crystallized framework and a low background indicating the absence of amorphous phase in the synthesized zeolite. The spectrum contained relatively large peaks at 6^O, 23^O and 45^O. The XRD analysis indicated that the crystals synthesized were single-phase ZSM-5 without any crystalline impurity phases. The SAR was also found to be 194.4 through the chemical composition analysis. High SAR value indicates that the exhibits high adsorption and catalytic property. Fig. 2 shows the SEM image of the ZSM-5 zeolites crystals. This is also in conformity with the reports of [19]. White crystals observed could be as a result of low-water synthesis employed. similarly reported that low-water of $H_2O:SiO_2 < 10$, in the presence of Fluoride was found to produce better siliceous zeolites unlike the conventional aluminosilicate zeolite syntheses that use $H_2O:SiO_2 > 25$ though it allow easy homogenization and handling of the synthesis gels. Crystal size was found to be between 200 – 218 µm while the BET surface area which was estimated using low nitrogen adsorption data revealed that the crystals have 628 m^2/g. The micropore volume was also estimated to be 0.79 cm^3/g. These values are somewhat close to the values usually gotten when surfactant liquid crystal is used as template in the synthesis process [4].

Figs. 3 to 6 show the results of the batch adsorption for COD and Fe. The reference levels of the contaminants being considered were found to be 1100 mg/l COD and 5.5 mg/l Fe. These contaminant levels are far higher than the limit of 40 mg/l COD and 1.0 mg/l Fe as regulated by [27]. The high content of the Fe could be attributed to the high iron content in Nigerian soils and probably due to the operative chemicals used in the various unit operations in the treatment of crude oil.

In Fig. 3, 5 and 6, the percent removal of the two contaminants increased steadily as the dosage was increased from 20 mg to 100 mg but the uptake decreased with increasing adsorbent dosage from 100mg. This may be attributed to many factors such as availability of solute, interference between binding sites, electrostatic interactions, and reduced mixing due to high adsorbent concentration in the solution. Many of the adsorption sites, therefore, remain unsaturated due to the limited availability of the sorbate, which in turn lowers the uptake and the adsorption efficiency. This is an indication that 100 mg was suitable to be considered as optimum dose. It was also observed that adsorption time has effect on the adsorption efficacy of the ZSM-5 zeolite on COD and Fe removal. Fig. 4 shows that the adsorption rate for Fe was doubly higher than that of COD in the first 10 minutes as it exhibited 53% removal while that of COD was just 24% removal. Surprisingly, equilibrium was reached at 80 minutes of contact and at 99% COD and 98% Fe removals. This indicates that the organic removal capacity has been improved through the synthetic procedures. These excellent performances is as a result of high adsorption capacity due the reduction in the hydrophilicity of the adsorbent which increases its organic removals present in the wastewater, the stability of the structure even after a prolonged immersion in water, the possibility of regenerating their initial sorption capacity by simple thermal treatment [7].

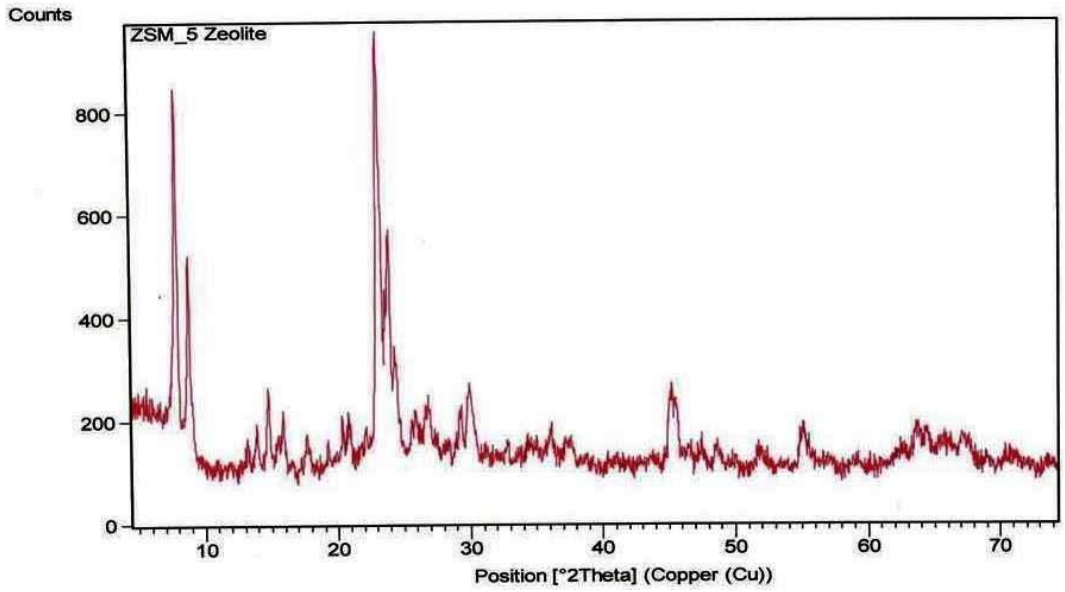

Fig. 1: XRD analysis showing the pattern of the synthesized ZSM-5

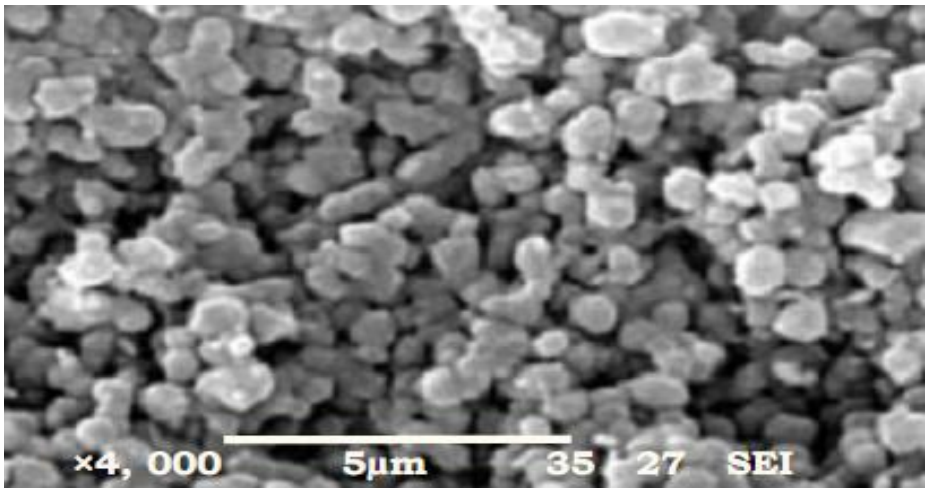

Fig. 2: SEM analysis showing the image of the synthesized ZSM-5 crystals

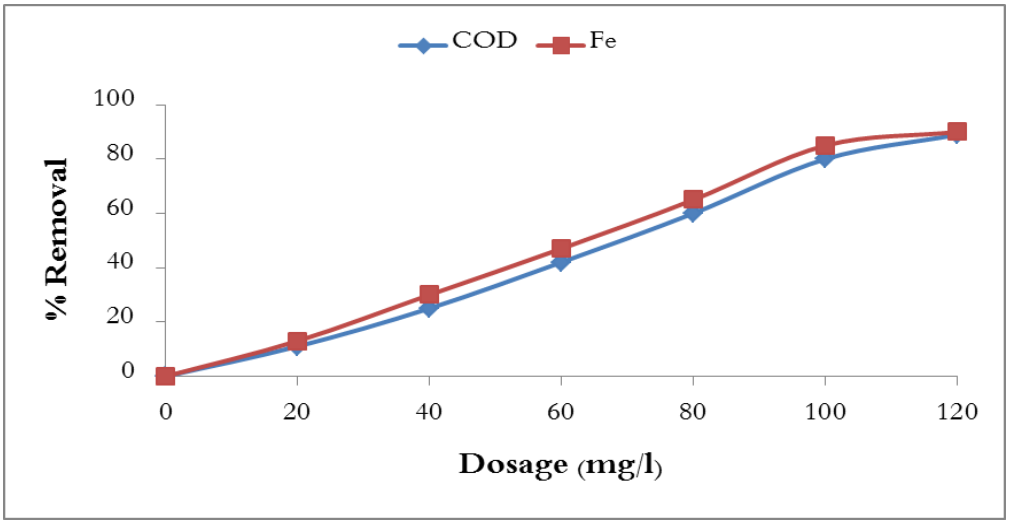

Fig. 3: Effect of zeolite dosage on the percentage removal of COD and Fe

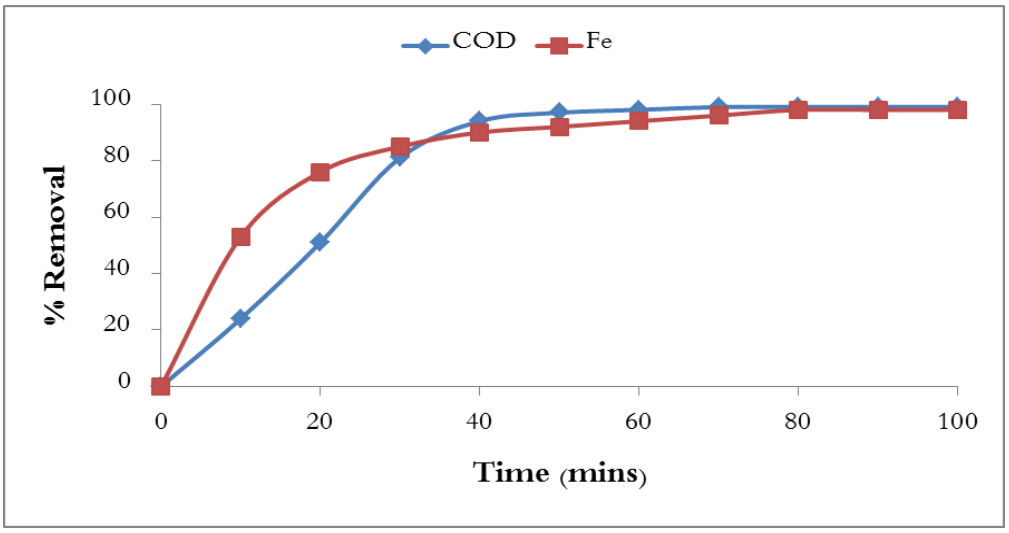

Fig. 4: Percentage removal of COD and Fe with time at zeolite dose 100mg.

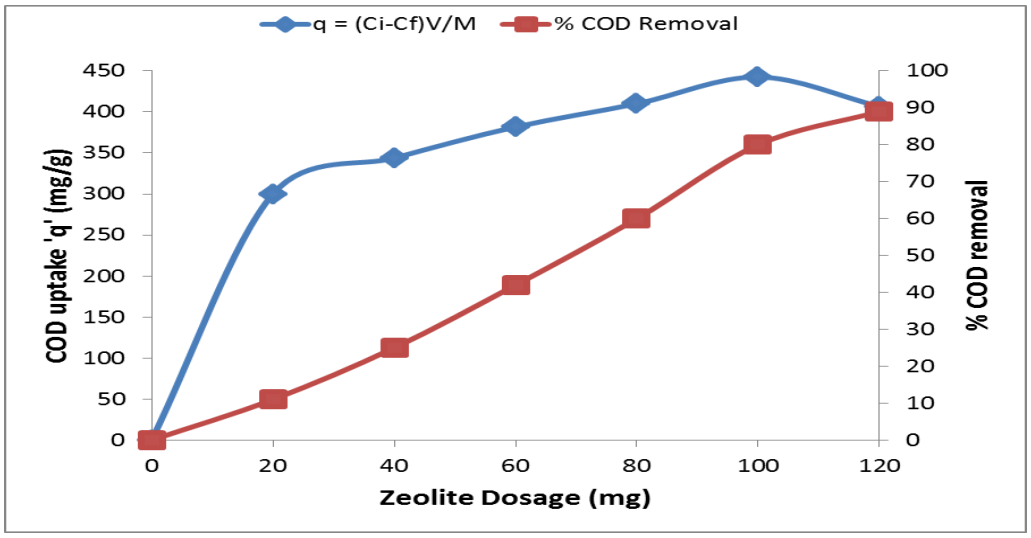

Fig. 5: Effect of zeolite dose on COD uptake.

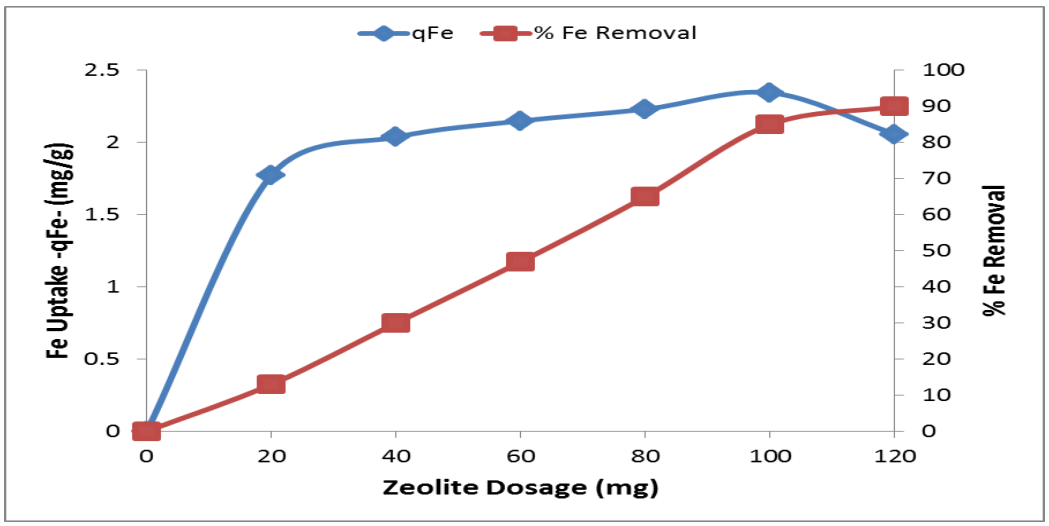

Fig. 6: Effect of zeolite dose on Fe uptake.

Sorption Isotherms:

Adsorption isotherm indicates how the molecules subjected to adsorption are distributed between the liquid and solid phases when the adsorption process reaches an equilibrium state. Furthermore, the analysis of the isotherm data by fitting them to different isotherm models is an important step in finding the suitable model that can be used for design purposes [32]. Due to this, four isotherm models (Langmuir, Freundlich, Temkin and Dubinin-Radushkevich (D-R)) have been employed in carrying out the isotherm studies in this study. All values for the determined parameters alongside their respective R^2 for each regression are presented in Table 2 and the results indicate that the experimental data were best fit by the Langmuir model for both COD and Fe removals because the R^2 values of for the Langmuir isotherm are significantly higher than those of other isotherms. Also, the values of R_L between 0 and 1 are an indication that the adsorption processes are favorable for both COD and Fe.

The basic assumption in the Langmuir theory is that adsorption takes place at specific homogenous sites within the adsorbent following the mathematical relation thus in Eq. 1 [33]:

$$\frac{C_e}{q_e} = \frac{1}{bQ_o} + \frac{C_e}{Q_o} \tag{1}$$

where q_e is the amount of COD or Fe adsorbed in mg/g, C_e is the equilibrium concentration (mg/l), b is the adsorption equilibrium constant (l/mg) and Q_o is the maximum adsorption capacity. A plot of C_e/q_e versus C_e gives the adsorption coefficients.

Furthermore, the Freundlich isotherm is derived by assuming a heterogenous surface with a non-uniform distribution of heat of adsorption over the surface. Freundlich equation is mathematically expressed as shown Eq. 2 [34]:

$$\log\ q_e = \log k_f + \frac{1}{n}\log C_e \tag{2}$$

where k_f and n are the Freundlich constants which represent adsorption capacity and adsorption intensity, respectively. The Freundlich constants were determined from the slope and intercept of a plot of log q_e versus log C_e.

When the Freundlich isotherm is considered, the values of n greater than unity indicate favorable nature of adsorption despite its relatively low R^2 values when compared with Langmuir isotherm [34].

The Temkin isotherm on the hand can be expressed in linear mathematical form thus in Eq. 3 [34]:

$$q_e = b \ln A + B \ln C_e \tag{3}$$

where B=RT/b, A is the equilibrium building constant (l/mg), B is related to the heat of adsorption. A plot of q_e versus ln C_e gives the respective isotherm constants.

The fourth isotherm model applied in this study is the Dubinin-Radushkevich (D-R) isotherm given by the linear mathematical relation shown in Eq. 4 [35]:

$$q_e = q_D \exp\left(-B_D\left[RT\ \ln\left(1+\frac{1}{C_e}\right)\right]^2\right) \tag{4}$$

where q_D is the D-R isotherm constant related to the degree of sorbate sorption by the sorbent surface (mg/g) and B_D is related to the free energy of sorption per mole of sorbate as it migrates to the surface of the adsorbent from infinite distance in the solution (mol^2/KJ^2). This means free energy can be estimated from the value of B_D using Eq. 5:

$$E = \frac{1}{\sqrt{2B_D}} \tag{5}$$

Figs. 7 through 14 show the plot of all the aforementioned isotherms.

Table 2: Isotherm parameters for removal of COD and Fe

Langmuir isotherm				
Parameter	Q_o	b	R_L	R^2
COD	151.52	0.025	0.038	0.8975
Fe	1.48	7.089	0.026	0.9725
Freundlich isotherm				
Parameter	n	k_f	R^2	
COD	7.675	255.92	0.2005	
Fe	8.489	2.688	0.4827	
Temkin isotherm				
Parameter	B	A	R^2	
COD	44.87	5.60E+02	0.2505	

Fe	0.2577	3.30E+04	0.5547	
D-R isotherm				
Parameter	q_D (mg/g)	B_D	E (KJ/mol)	R^2
COD	321.85	3.26E-12	391.6	0.3481
Fe	2.07	1.47E-15	1.84E+04	0.427

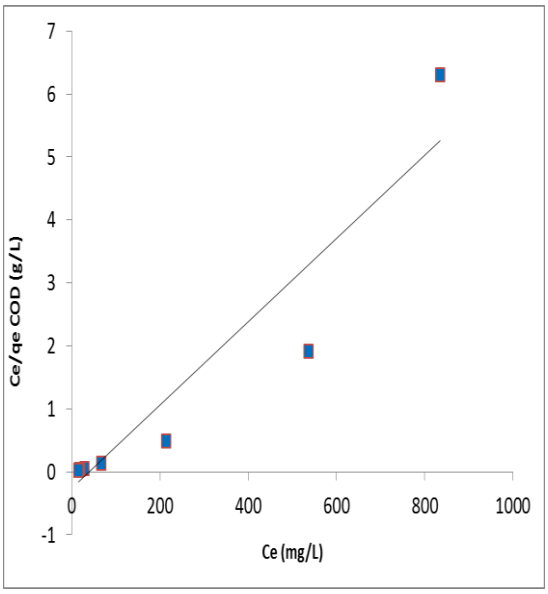

Fig. 7: Langmuir model "C_e/q_e vs. C_e" for COD

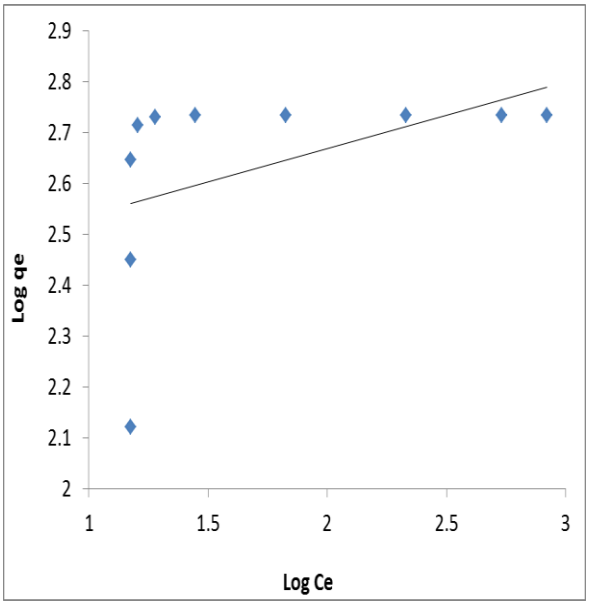

Fig. 8: Freundlich model "$\log q_e$ vs. $\log C_e$" for COD

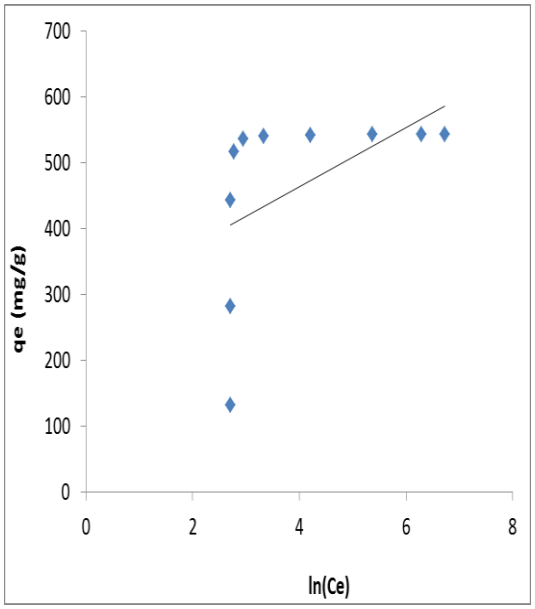

Fig. 9: Temkin model "q_e vs. $\ln(C_e)$" for COD

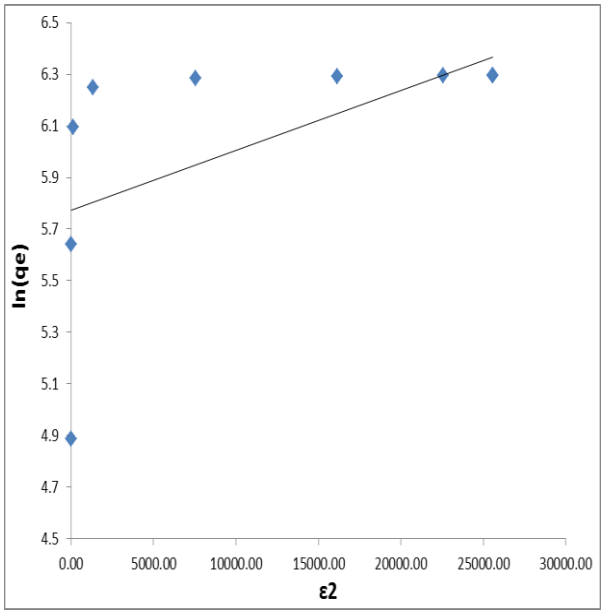

Fig. 10: D-R model "$\ln(q_e)$ vs. ε^2" for COD

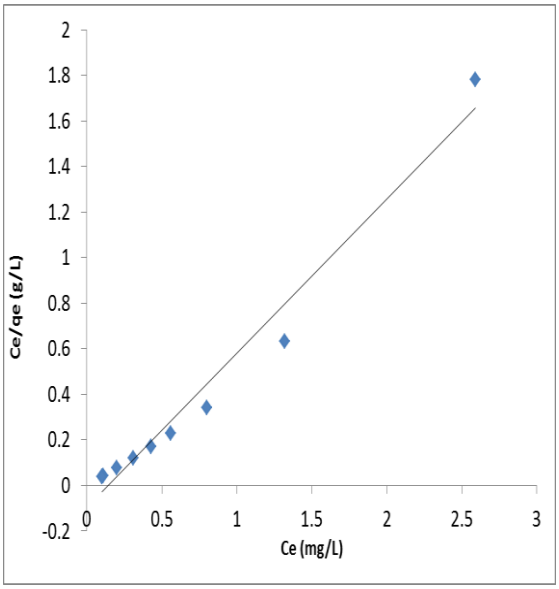

Fig. 11: Langmuir model "C_e/q_e vs. C_e" for Fe

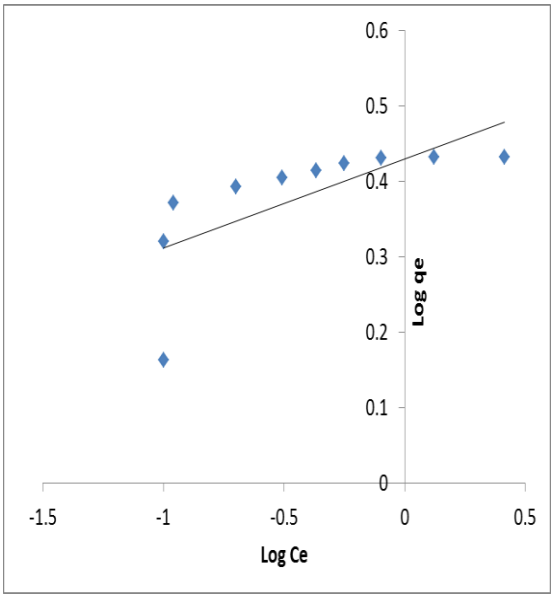

Fig. 12: Freundlich model "$Logq_e$ vs. Log C_e" for Fe

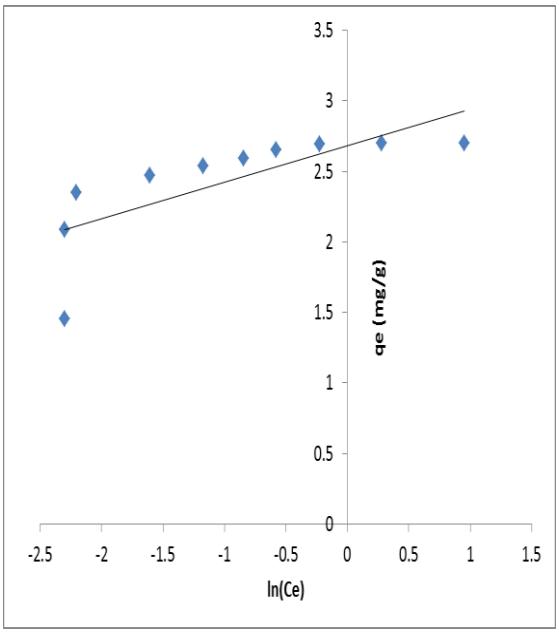

Fig. 13: Temkin model "q_e vs. $\ln(C_e)$" for Fe

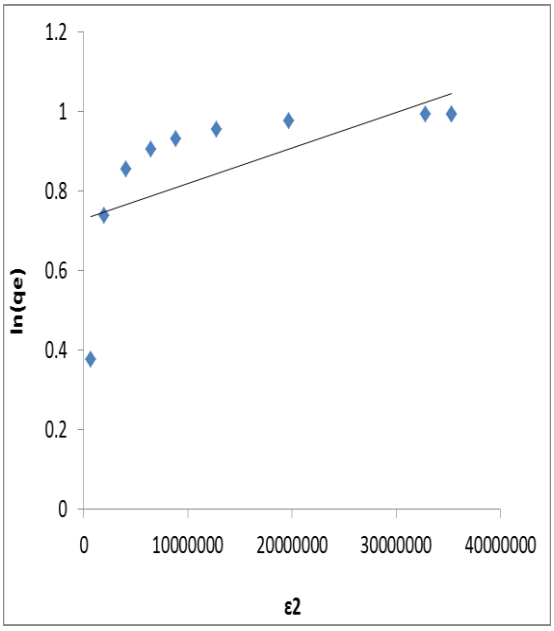

Fig. 14: D-R model "$\ln(q_e)$ vs. ε^2" for Fe

Sorption Kinetics:

The controlling mechanism of the adsorption process was studied using four kinetic models. Pseudo-first-order, pseudo-second-order, Elovich and Intra-particle diffusion models were the kinetics models employed in testing the experimental data.

The Lagergren pseudo-first-order model is most commonly used to describe the adsorption of solute from a liquid solution. A simple kinetic analysis of its linearized differential equation is usually given as depicted in Eq. 6:

$$\log(q_e - q_t) = \log q_e - \frac{k_1 t}{2.303} \quad (6)$$

where qe and q_t are the amounts of COD and Fe adsorbed (mg/g) at equilibrium and at time t (min), respectively, and k_1 (l/min) is the rate constant of first-order adsorption.

The pseudo-second order model can as well be expressed in the linearized form as shown in Eq. 7 [36]:

$$\frac{t}{q_t} = \frac{1}{k_2 q_e^{\,2}} + \frac{t}{q_e} \quad (7)$$

where k_2 is the pseudo-second-order rate constant (g/mg min), q_e and q_t are the amounts of COD or Fe adsorbed (mg/g) at equilibrium and at time t (min), respectively.

Besides, Elovich's model has been used in the recent years to describe the adsorption of pollutants from aqueous solutions applying the linearized form of the model given in Eq. 8:

$$q = \frac{1}{b}\ln(ab) + \frac{1}{b}\ln(t) \quad (8)$$

where a is the initial adsorption rate (mg/g/min), and $1/b$ (mg/g) is a parameter related to the number of sites available for adsorption.

The fact that adsorption is a multi-step process involving transport of the solute molecules from the aqueous phase to the surface of the solid particles followed by diffusion into the interior of the pores necessitated the application of intra-particle diffusion model in this study. The model equation is given in Eq. 9 thus [37]:

$$q_t = k_p t^{1/2} \quad (9)$$

where k_p is the intra-particle rate constant (g/mg/min$^{1/2}$).

The fit of all the aforementioned kinetic models was checked by their respective linear plots (Figs. 15 through 22), bringing about the determination of their parameters, and by comparing the regression coefficients of each expression. The rate constants, calculated equilibrium uptakes and the corresponding correlation coefficients were given in Table 3.

Table 3: Kinetic parameters for adsorption rate expressions

Pseudo-first order			
Parameter	q_e (mg/g)	k (/min)	R^2
COD	1231.4	0.2411	0.964
Fe	2.8098	0.1499	0.9202
Pseudo-second order			
Parameter	q_e (mg/g)	k (g/mg.min)	R^2
COD	769.23	1.54E+07	0.9176
Fe	2.853	0.0617	0.9952
Elovich's equation			
Parameter	a (mg/g/min)	$1/b$ (mg/g)	R^2
COD	91.47	137.19	0.9037
Fe	0.728	1.659	0.9767
Intra-particle Diffusion Model			
Parameter	k_d	R^2	
COD	60.044	0.8733	
Fe	0.2502	0.8487	

The correlation coefficient which is closest to unity in the case of COD adsorption is that of the pseudo-first-order model, therefore the adsorption kinetic could well be approximated more favorably by the model. Whereas in the case of Fe adsorption, the pseudo-second-order model was most fit as it gave the highest R^2 value with especially the calculated q_e value which is in good agreement with the experimental results for second-order kinetic model.

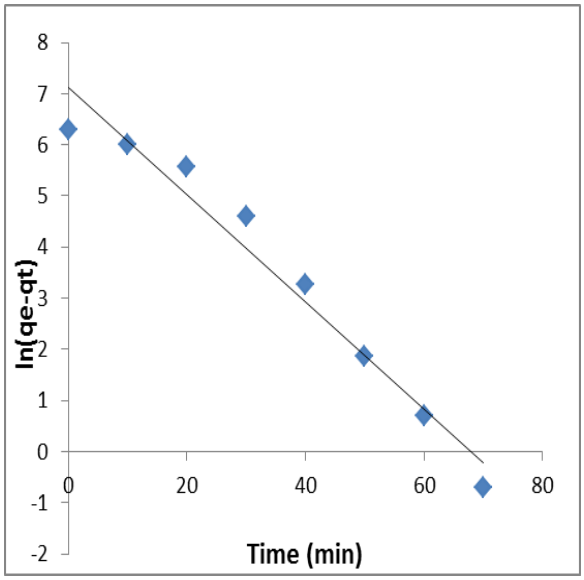

Fig. 15: Pseudo-first-order model "$\ln(q_e-q_t)$ vs. t" for COD

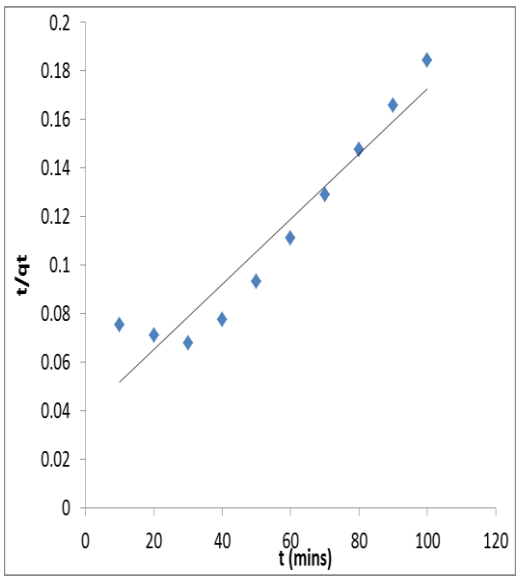

Fig. 16: Pseudo-second-order model "t/q_t vs. t" for COD

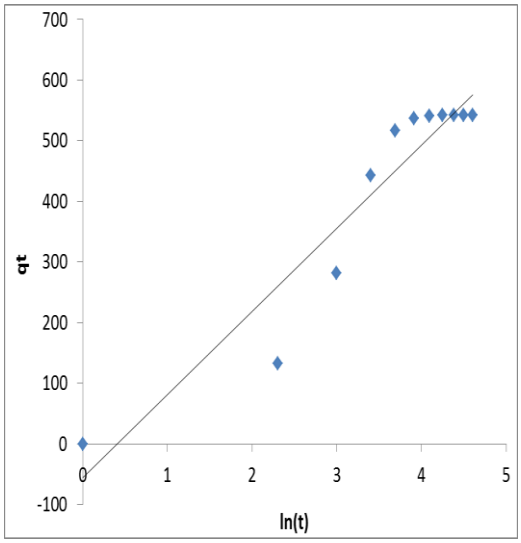

Fig. 17: Elovich model "q_t vs. ln(t)" for COD

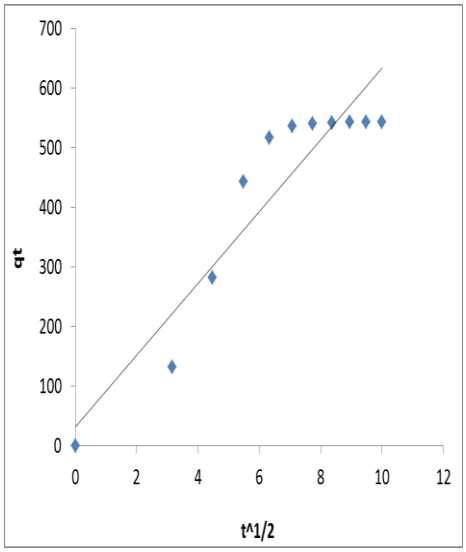

Fig. 18. Intra-particle diffusion model "q_t vs. $t^{1/2}$" for COD

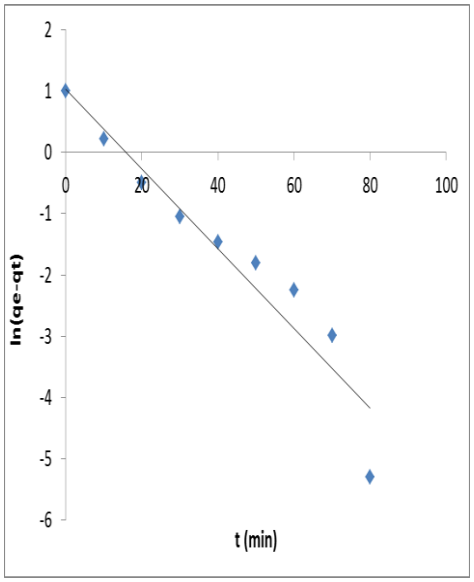

Fig. 19: Pseudo-first-order model "$\ln(q_e-q_t)$ vs. t" for Fe

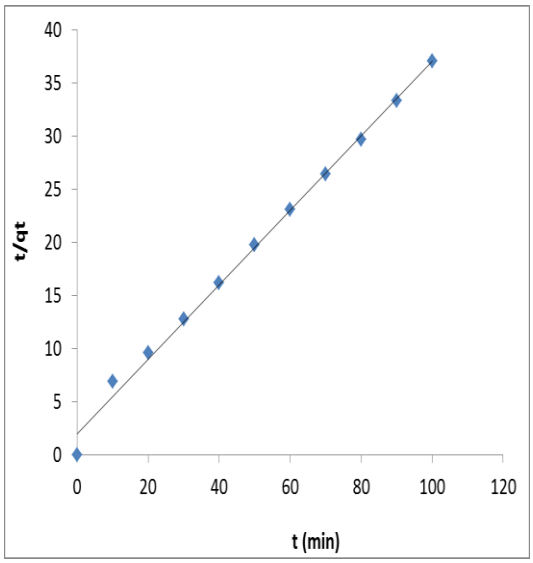

Fig. 20: Pseudo-second-order model "t/q_t vs. t" for Fe

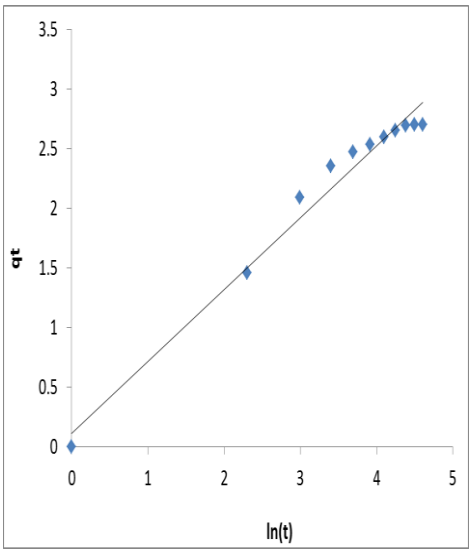

Fig. 21: Elovich model "q_t vs. ln(t)" for Fe

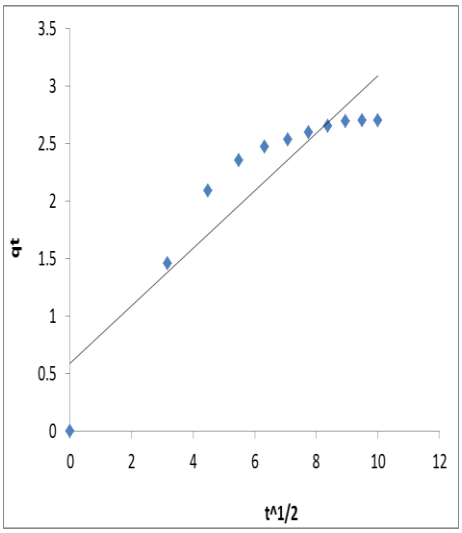

Fig. 22: Intra-particle diffusion model "q_t vs. $t^{1/2}$" for Fe

Conclusions:

This present study has revealed the possibility of a purpose-tailored zeolite (ZSM-5) for better adsorptive and shape selectivity capacities using low-water and fluoride methods of synthesis simultaneously. Characterization of the synthesized zeolite was found to be in line with the verified zeolite frameworks [30,31].

The study further revealed that the effluent from the petroleum processing industry has high pollution potentials and that synthetic zeolite ZSM-5 adsorption is an efficient method for its treatment due to high sorption capacity possessed by the zeolite. The high removal efficiency for both organic (COD) and inorganic (Fe) pollutants exhibited by the zeolite may be attributed to its high purity, uniform and well compartmentalized intracrystalline pores resulting from its high surface area and micropore volumes.

The isotherm study performed on the synthesized zeolite adsorption revealed that Langmuir isotherm fitted best for the description of both organic (COD) and inorganic (Fe) adsorption processes. Likewise, the kinetic study performed revealed that the pseudo-first-order model fitted best for organic (COD) adsorption where the pseudo-second-order fitted for the inorganic (Fe) adsorption.

These advantages surely compensate the higher costs of the materials with respect to the conventional adsorbents (e.g. PAC, GAC and natural zeolites), rendering the technologies based on zeolites appealing for future applications.

REFERENCES

[1] Obire, O. and F. Amusan, 2004. The Environmental impact of oilfield formation water on a freshwater stream in Nigeria. Journal of Applied Sciences and Environmental Management, 7(1): 61-66.
[2] UNDP, 2006. Niger Delta human development report. United Nations Development Programme
[3] Amnesty International, 2009. Petroleum, Pollution and Poverty in the Niger Delta.
[4] Kulprathipanja, S., 2010. Zeolites in industrial separation and catalysis. Wiley Online Library.
[5] Cejka, J., A. Corma and S. Zones, 2010. Zeolites and Catalysis: Synthesis, Reactions and Applications. WILEY-VCH Verlag GmbH & Co. KGaA.
[6] Vermeiren, W. and J.-P. Gilson, 2009. Impact of zeolites on the petroleum and petrochemical industry. Top. Catal., 52(9): 1131-1161.
[7] Cejka, J., H. Van Bekkum, A. Corma and F. Schüth, 2007. Introduction to Zeolite Science and Practice, In Studies in Surface Science and Catalysis 168. Elsevier BV
[8] Ghamami, M. and L. Sand, 1983. Synthesis and crystal growth of zeolite-ZSM-5. Zeolites, 3(2): 155-162.
[9] Derouane, E.G. and Z. Gabelica, 1986. Role of selected synthesis variables in nucleation and growth of zeolite ZSM-5. J. Solid State Chem., 64(3): 296-304.
[10] Di Renzo, F., 1998. Zeolites as tailor-made catalysts: control of the crystal size. Catal. Today, 41(1): 37-40.
[11] Coker, E.N., J.C. Jansen, F. DiRenzo, F. Fajula, J.A. Martens, P.A. Jacobs and A. Sacco, 2001. Zeolite ZSM-5 synthesized in space: catalysts with reduced external surface activity. Microporous Mesoporous Mater., 46(2): 223-236.
[12] Gao, F., G. Zhu, X. Li, B. Li, O. Terasaki and S. Qiu, 2001. Synthesis of a high-quality host material: Zeolite MFI giant single crystal from monocrystalline silicon slice. The Journal of Physical Chemistry B, 105(51): 12704-12708.
[13] Ke, J.-A. and I. Wang, 2001. Elucidation of the role of potassium fluoride in the chemical and physical nature of ZSM-5 zeolite. Mater. Chem. Phys., 68(1): 157-165.
[14] Nair, S., L.A. Villaescusa, M.A. Camblor and M. Tsapatsis, 1999. Zeolite-b grown epitaxially on SSZ-31 nanofibers. Chem. Commun, 921: 922.
[15] Na, K., C. Jo, J. Kim, K. Cho, J. Jung, Y. Seo, R.J. Messinger, B.F. Chmelka and R. Ryoo, 2011. Directing zeolite structures into hierarchically nanoporous architectures. Science, 333(6040): 328-332.
[16] Wu, P., D. Nuntasri, J. Ruan, Y. Liu, M. He, W. Fan, O. Terasaki and T. Tatsumi, 2004. Delamination of Ti-MWW and high efficiency in epoxidation of alkenes with various molecular sizes. The Journal of Physical Chemistry B, 108(50): 19126-19131.
[17] Follens, L., A. Aerts, M. Haouas, T. Caremans, B. Loppinet, B. Goderis, J. Vermant, F. Taulelle, J. Martens and C.E. Kirschhock, 2008. Characterization of nanoparticles in diluted clear solutions for Silicalite-1 zeolite synthesis using liquid 29Si NMR, SAXS and DLS. Phys. Chem. Chem. Phys., 10(36): 5574-5583.
[18] Chen, X., W. Yan, X. Cao, J. Yu and R. Xu, 2009. Fabrication of silicalite-1 crystals with tunable aspect ratios by microwave-assisted solvothermal synthesis. Microporous Mesoporous Mater., 119(1): 217-222.
[19] Xu, R., W. Pang, J. Yu, Q. Huo and J. Chen, 2009. Chemistry of zeolites and related porous materials: synthesis and structure. John Wiley & Sons.
[20] Kawai, T. and K. Tsutsumi, 1994. The appearance of adsorption ability of modified zeolites for sodium dodecylsulfate from its aqueous solution. Colloid Polym. Sci., 272(7): 830-836.
[21] Li, S., V.A. Tuan, R.D. Noble and J.L. Falconer, 2003. MTBE adsorption on all-silica β zeolite. Environ. Sci. Technol., 37(17): 4007-4010.

[22] International Zeolite Association, 2013. Database of Zeolite Structures.
[23] Weitkamp, J. and L. Puppe, 1999. Catalysis and zeolites: fundamentals and applications. Springer.
[24] Weitkamp, J., 2000. Zeolites and catalysis. Solid State Ionics, 131(1): 175-188.
[25] Vignola, R., G. Grillo, R. Sisto, G. Capotorti, P. Cesti and M. Molinari, 2005. Synthetic zeolites as sorbent material for PRBs at industrially contaminated sites. IAHS PUBLICATION, 298: 105.
[26] Vignola, R., U. Cova, F. Fabiani, G. Grillo, M. Molinari, R. Sbardellati and R. Sisto, 2008. Remediation of hydrocarbon contaminants in groundwater using specific zeolites in full-scale pump&treat and demonstrative permeable barrier tests. Stud. Surf. Sci. Catal., 174: 573-576.
[27] Department of Petroleum Resources, 1991. Environmental Guidelines and Standards for the Petroleum Industry in Nigeria. Brady N.C.
[28] APHA, AWWA and WPCF, 2005. Standard Methods for the Examination of Water and Wastewater. American Public Health Association.
[29] Golterman, H., R. Clymo and M. Ohnstad, 1978. IBP handbook-Methods for physical and chemical analysis of fresh waters. 2nd Edn., Blackwell.
[30] NaRobson, H., 2001. Verified Syntheses of Zeolitic Materials. Second Revised Edn., Elsevier Science B.V.
[31] Baerlocher, C., L.B. McCusker and D.H. Olson, 2007. Atlas of Zeolite Framework Types. 6th Revised Edn., Elsevier B. V.
[32] Demiral, H. and G. Gündüzoğlu, 2010. Removal of nitrate from aqueous solutions by activated carbon prepared from sugar beet bagasse. Bioresour. Technol., 101(6): 1675-1680.
[33] Demiral, H., İ. Demiral, F. Tümsek and B. Karabacakoğlu, 2008. Pore structure of activated carbon prepared from hazelnut bagasse by chemical activation. Surf. Interface Anal., 40(3-4): 616-619.
[34] Hameed, B. and F. Daud, 2008. Adsorption studies of basic dye on activated carbon derived from agricultural waste: Hevea brasiliensis seed coat. Chem. Eng. J. (Lausanne), 139(1): 48-55.
[35] Ho, Y., J. Porter and G. McKay, 2002. Equilibrium isotherm studies for the sorption of divalent metal ions onto peat: copper, nickel and lead single component systems. Water, Air, Soil Pollut., 141(1-4): 1-33.
[36] Amin, N.K., 2008. Removal of reactive dye from aqueous solutions by adsorption onto activated carbons prepared from sugarcane bagasse pith. Desalination, 223(1): 152-161.
[37] Acharya, J., J. Sahu, C. Mohanty and B. Meikap, 2009. Removal of lead (II) from wastewater by activated carbon developed from Tamarind wood by zinc chloride activation. Chem. Eng. J. (Lausanne), 149(1-3): 249-262.